Available online at www.sciencedirect.com
SCIENCE DIRECT®

Journal of the European Ceramic Society 24 (2004) 2951–2958

www.elsevier.com/locate/jeurceramsoc

Ferroelectric glass-ceramics from the $PbO–GeO_2–Nb_2O_5$ system

K. Pengpat[a], D. Holland[b,*]

[a]*Department of Physics, Faculty of Science, Chiang Mai University, Chiang Mai 50200, Thailand*
[b]*Department of Physics, University of Warwick, Coventry CV4 7AL, UK*

Received 22 August 2003; received in revised form 6 November 2003; accepted 8 November 2003

Abstract

Glass-ceramics with compositions $Pb_5Ge_3O_{11}–xPbNb_2O_6$ (PG–*x*PN) where x equals 0.0, 0.5, 1, 2 and 3, and other selected compositions from the $PbO–GeO_2–Nb_2O_5$ system, have been prepared using the conventional melt-quench method. Most of the quenched melts devitrified on cooling and gave fragile samples. The $x=0.5$ (PGN2) sample formed a robust solid which contained the ferroelectric phase $Pb_5Ge_3O_{11}$ and the pyrochlore phase $Pb_2Nb_2O_7$. Glass formation was improved by replacing some Nb_2O_5 by GeO_2. Scanning electron micrographs of cross-sections of the $x=0.5$ sample showed surface crystallisation of the PG phase with a-axis orientation. The PN phase was distributed randomly in the sample. Heating the sample at 667 °C for 48 h enhanced the surface orientation of this PG phase. After poling the heat treated sample, using an electric field of up to 25 kV/cm, a ferroelectric hysteresis loop could be obtained at room temperature with $Ps=1$ μC/cm^2. The Curie point of this PGN2 sample was found to be ~166 °C.

Keywords: Dielectric properties; Ferroelectric properties; Glass ceramics; Microstructure; $Pb_5Ge_3O_{11}$; $Pb_2Nb_2O_7$

1. Introduction

As a result of its high electronic polarisability, the Pb^{2+} ion plays an important role in many commercial ferroelectric materials, such as $Pb(Zr_{1/2}Ti_{1/2})O_2$, $PbTiO_3$ and $PbNb_2O_6$. $Pb_5Ge_3O_{11}$ (PG) is one of the important ferroelectric phases to emerge during the past few decades. It has a low processing temperature and many possible applications, for example: pyroelectric sensors and nonvolatile ferroelectric memories.[1] The ferroelectric properties of the PG single crystals were independently discovered by Iwasaki and Sugii[2] and Nanamatsu et al[3] in 1971. Since then many research groups have produced different forms of $Pb_5Ge_3O_{11}$-based ferroelectric materials with high transparency such as single crystals, thin and thick films and glass-ceramics.[1–12]

As this PG phase already contains a good glass former (GeO_2), attention has been paid to the glass-ceramic method as a fabrication route. However, the stoichiometric composition of this phase ($5PbO:3GeO_2$) is very close to the glass-forming boundary, therefore the corresponding glasses have a tendency to crystallise during the glass-quenching method. As a result, studies have concentrated on adding other oxides to the PG phase, such as glass formers to ease glass formation,[13–16] or ferroelectric phases to improve the ferroelectric properties.[12]

Hasegawa et al.[16] added the glass former SiO_2 to the PG phase and found that they could prepare glass-ceramics which were transparent, with crystals of the solid solution phase $Pb_5Ge_{3-x}Si_xO_{11}$ being less than 300 nm in size. Moreover, the SiO_2 addition not only stabilised glass formation but also reduced the Curie point of the PG ceramics. Some groups have tried to add an additional ferroelectric phase to the PG in order to produce multiple ferroelectric glass-ceramics. For example, glass compositions in the $Pb_5Ge_3O_{11}–PbTiO_3$ (PG–PT) and $Pb_5Ge_3O_{11}–Pb(Zr_{1/2}Ti_{1/2})O_3$ (PG–PZT) systems were investigated by Cornejo and Haun [12] who found that the addition of PT and PZT enhanced the electrical properties of the materials.

In this work, a new ferroelectric glass-ceramic system, $Pb_5Ge_3O_{11}–PbNb_2O_6$, is reported. The lead niobate ($PbNb_2O_6$) addition was chosen because it is an important commercial ferroelectric ceramic with excellent piezoelectric properties.

* Corresponding author.
E-mail address: d.holland@warwick.ac.uk (D. Holland).

0955-2219/$ - see front matter © 2003 Elsevier Ltd. All rights reserved.
doi:10.1016/j.jeurceramsoc.2003.11.017

2. Experimental procedure

Glasses of the nominal compositions given in Table 1 were prepared from the $PbO–GeO_2–Nb_2O_5$ system. Compositions PGN1 to PGN5 correspond to $Pb_5Ge_3O_{11}–xPbNb_2O_6$ (PG–*x*PN) ($x = 0.0$, 0.5, 1, 2, 3) whilst the subsequent compositions are aimed at improving glass stability. The starting materials were reagent-grade red lead oxide (Pb_3O_4), 99% germanium oxide (GeO_2) and 99.5% niobium(V) oxide (Nb_2O_5). A 30 g batch of the starting materials for each composition was mixed in an agate pestle and mortar for 20 min and then melted, in a 90Pt/10Rh crucible, in an air atmosphere, using an electric furnace. The melting temperatures were in the range 1000–1150 °C. After holding at the melting temperature for 15 to 30 min, each melt was splat-quenched between copper plates at either room temperature or liquid-nitrogen. The thermal properties of selected samples were investigated using Differential Thermal Analysis (DTA) with a Stanton Redcroft DTA model 673-4, employing a heating rate of 10 °C min^{-1} and with quartz as the reference. The quartz reference provides a reversible, sharp, $\alpha \leftrightarrow \beta$ transition with an onset temperature on cooling of 573 °C, thus providing both a temperature reference and a confirmation of the exothermic/endothermic directions. Some glasses were subjected to heat treatment schedules for crystallisation with heating and cooling rates of 5 °C min^{-1} and 10 °C min^{-1} respectively and with 4 h dwell at the crystallisation temperature. A Philips powder diffractometer with Cu K_α ($\lambda = 1.54178$ Å) radiation was used to identify the phase composition in the glass-ceramics. The microstructures of selected glass-ceramics were observed using a Jeol 6100 scanning electron microscope (SEM) in back-scattered electron mode and Energy Dispersive X-ray (EDX) analysis was performed for phase identification of individual features. The dielectric constants (ε_r') and dissipation factors (ε_r'') were measured at 10 kHz, 100 kHz and 1 MHz for selected samples from room temperature up to 500 °C using a high temperature rig and LCR meter (Hewlett-Packard 4192A LF Impedance Analyser). Ferroelectric hysteresis loops were measured using a modified Sawyer–Tower circuit[17] with compensation added[18] and input voltages in the range of 1–1.5 kV at 50–100 Hz. The samples were polished to ~0.3 mm thickness and silver-paste electrodes of 2 mm diameter were applied on both sides of the samples.

Table 1
Nominal glass compositions in mol%. The numbers in brackets correspond with the composition labelling in Fig. 1

Sample	PbO (mol%)	GeO_2 (mol%)	Nb_2O_5 (mol%)
PGN1 (1)	62.5	37.5	0
PGN2 (2)	61.1	33.4	5.5
PGN3 (3)	60	30	10
PGN4 (4)	58.3	25	16.7
PGN5 (5)	57.2	21.4	21.4
PGN6 (6)	56.9	37.6	5.5
PGN7 (7)	52.5	42	5.5
PGN8 (8)	47.5	47	5.5
PGN9 (9)	51.4	38.6	10
PGN10 (10)	50	35	15

3. Results and discussion

3.1. Glass formation

3.1.1. PGN1

This is the $5PbO:3GeO_2$ stoichiometric composition which lies just at the edge of the glass forming region[19] as shown in Fig. 1. It gave a melt of noticeably low viscosity, as reported by Cornejo and Haun[12] and splat-quenching of the melt between liquid-N_2 cooled copper plates gave pieces of partially devitrified material about 0.5 mm thick. X-ray diffraction (Fig. 2) showed that the crystalline phase formed during quenching is $Pb_5Ge_3O_{11}$ (JCPDS No. 24-0576).

3.1.2. PGN2 to PGN5

These compositions, of nominal stoichiometry $Pb_5Ge_3O_{11}–xPbNb_2O_6$ (PG–*x*PN) ($x = 0.5$, 1, 2, 3), lie on the tieline between $Pb_5Ge_3O_{11}$ and $PbNb_2O_6$ as shown in Fig. 1. All melts had noticeably low viscosity, giving rise to crystallisation on quenching. The powder diffraction patterns of these samples are shown in Fig. 2 and Table 2 contains the crystal phase information as obtained by JCPDS comparison. It can be seen that, as the lead niobate content is increased, the sample becomes almost completely crystalline. From Fig. 1 it can be seen that the PGN4 and PGN5 samples are not in the reported glass formation region, which agrees

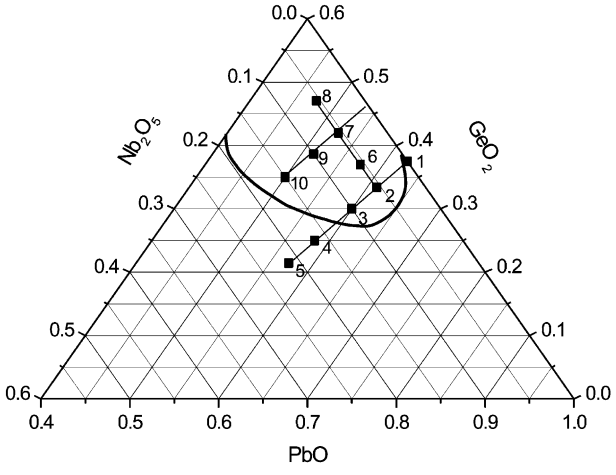

Fig. 1. Positions of the sample compositions in the $PbO–GeO_2–Nb_2O_5$ phase diagram and comparison with the glass forming region after Mazurin et al.[19]

with the devitrification observed and the difficulty in making glass from these compositions. Although samples PGN2 and PGN3 do lie in the reported glass formation region, it was still difficult to make glasses without devitrification using the conventional fast-quenching method. This could result from compositional change during melting, as lead oxide is fairly volatile. However, the observed weight losses were quite low, between 0.7 and 1.2 wt.%. In order to cope with this problem, a more rapid quenching technique is needed.[20] Another possible solution to the problem of glass stability is to add a small amount of either glass-forming oxide (GeO_2) or volatilised oxide (PbO) to the compositions and this led to the preparation of samples PGN6 to PGN10.

3.1.3. PGN6 to PGN10

Compositions PGN6 to PGN10 are shown in the ternary PbO–GeO_2–Nb_2O_5 diagram (Fig. 1) and are summarised in Table 1. Only PGN7 and PGN8 produced X-ray amorphous samples on quenching from the ~1000 °C melting temperature (Fig. 3), whilst the remaining compositions showed some devitrification, giving $Pb_2Nb_2O_7$ (JCPDS No. 40-829) and resulting in samples which fractured readily on handling.

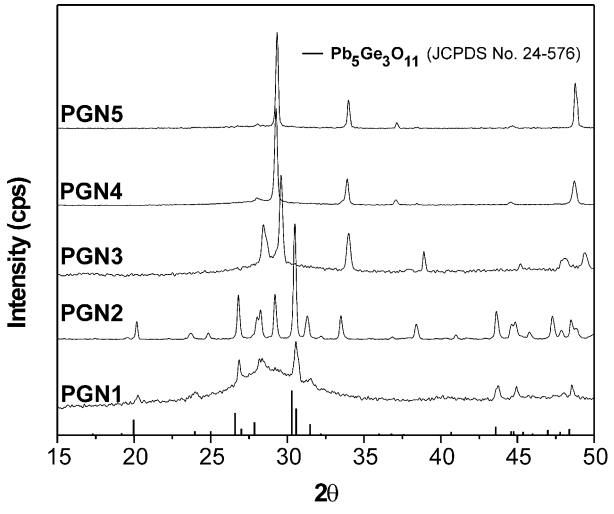

Fig. 2. X-ray diffraction patterns from as-quenched samples of compositions PGN1 to PGN5.

Table 2
Crystal phase information for as-quenched PGN1 to PGN5

Sample	Devitrification phase	JCPDS Number
PGN1	$Pb_5Ge_3O_{11}$	24-576
PGN2	$Pb_5Ge_3O_{11}$ & $Pb_2Nb_2O_7$	24-576 & 40-829
PGN3	$Pb_2Nb_2O_7$	43-960
PGN4	$Pb_5Nb_4O_{15}$	46-637
PGN5	$Pb_3Nb_4O_{13}$	25-443

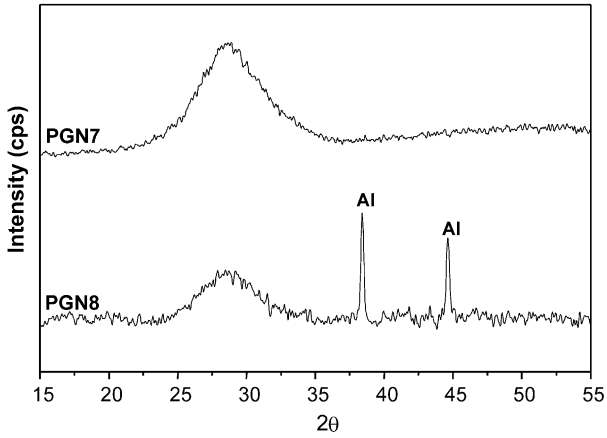

Fig. 3. X-ray diffraction patterns of as-quenched PGN7 and PGN8. Peaks labelled Al are from the aluminium sample holder.

3.2. Glass-ceramics

3.2.1. PGN2

Quenched samples of PGN1, PGN3, PGN4 and PGN5 were of limited use for property measurement since they had fragmented due to thermal shock. However, sample PGN2 yielded sizeable pieces of glass-ceramic and contained two interesting phases: $Pb_5Ge_3O_{11}$ and $Pb_2Nb_2O_7$. SEM backscattered electron images of a PGN2 cross-section and EDX spectra of the observed phases are shown in Fig. 4. Crystallites of $Pb_2Nb_2O_7$, from 1 to 10 μm in size, occur randomly throughout the sample and form the only crystal phase within ~21 μm of the base of the sample. In the region above this, for ~120 μm, these crystals are surrounded by a thin layer, about 0.5–1 μm, of $Pb_5Ge_3O_{11}$. This lead germanate phase also crystallises from the sample surface, growing to about 165 μm deep in the sample. This indicates that the $Pb_2Nb_2O_7$ phase nucleates homogeneously throughout the sample and $Pb_5Ge_3O_{11}$ subsequently nucleates and grows on the sample surface and the interfaces formed by the $Pb_2Nb_2O_7$ crystals. Surface crystallisation of $Pb_5Ge_3O_{11}$ has been observed in PG-based thick films by Cornejo and Haun who reported distinct c-axis orientation.[12] Only near the sample base, which was subject to the most rapid cooling, does the $Pb_5Ge_3O_{11}$ phase fail to grow. This glass-ceramic is a strong, pore-free material.

XRD patterns of the top and bottom surfaces are compared with a powdered sample in Fig. 5, confirming that the top surface contains both $Pb_5Ge_3O_{11}$ and $Pb_2Nb_2O_7$ while the bottom surface shows only $Pb_2Nb_2O_7$. The surface patterns also show the presence of significant glass phase near the two surfaces, consistent with them being in close contact with the quenching plates. The powder sample represents an average of the whole sample and it can be seen that no glass peak is visible on this scale. Closer examination shows that there may be as much as 10% glass phase

present but this still implies that the medium grey matrix phase in Fig. 4 must also be crystalline, consisting of smaller grains of $Pb_5Ge_3O_{11}$. This was confirmed by obtaining a DTA trace from the PGN2 quenched sample (Fig. 6). There is no detectable glass transition peak for this sample in the heating trace and the only other peak is that for the $\alpha \leftrightarrow \beta$ quartz transition from the reference. The lack of T_g and any exothermic peak confirms that crystallisation is nearly complete. However, Fig. 6 also shows that, on cooling from above the melting point, there is an exothermic peak at about 667 °C which is due to formation of $Pb_5Ge_3O_{11}$ from the melt. Therefore the PGN2 sample was heated at this temperature for 48 hrs in an attempt to induce crystal regrowth. XRD patterns from the surfaces of the heat-treated PGN2 sample are shown in Fig. 7 and can be compared with those from the as-cast sample in Fig. 5. It can be seen that devitrification and recrystallisation have combined to produce a surface crystallisation with specific orientation perpendicular to the (h00) planes, i.e. crystallographic *a*-axis orientation. This is different from the *c*-axis orientation observed in the PG-based thick films by Cornejo and Haun.[12] However, this recrystallised sample was also quite fragile.

3.2.2. PGN7 and PGN8

DTA traces from PGN7 and PGN8 glasses are shown in Fig. 8. From the DTA traces, it can be seen that the

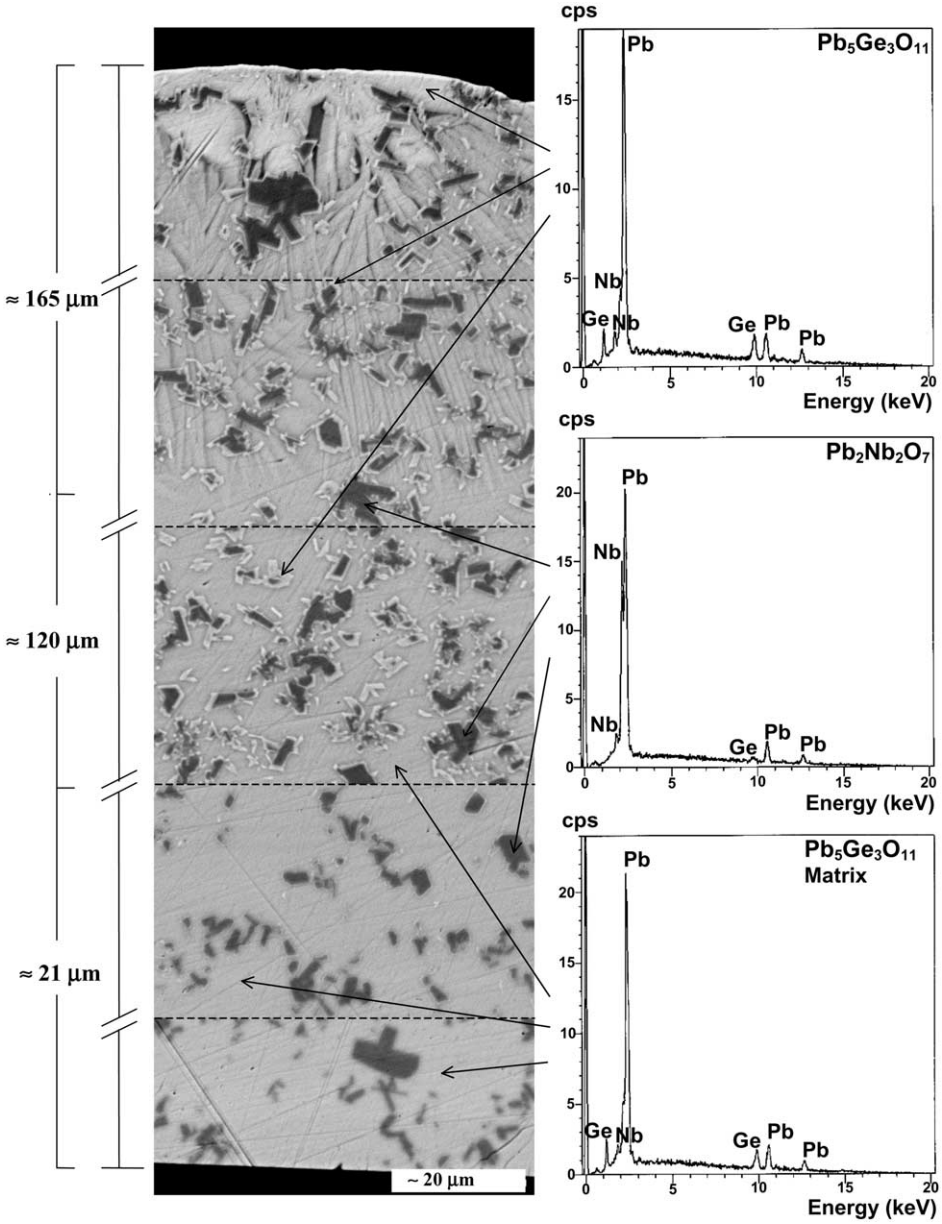

Fig. 4. Electron back-scattered image of a cross-section from an as-quenched sample of PGN2, 306 µm in thickness, with EDX spectra of the phases observed.

increased GeO_2 content reduces the melting temperature and enhances the stability of the PGN8 glass. It may be noted that the cooling trace of PGN8 has no α-β quartz transition because, during DTA analysis, this sample was heated to 1500 °C where β-quartz will transform to β-tridymite. However, the reverse transformation is slow so that β-tridymite is retained below the tridymite-quartz transition and eventually transforms to α-tridymite by the more rapid displacive phase transformation. This is seen as a negative going peak (=exothermic for the reference) at 220 °C in the PGN8 cooling trace. This was confirmed by XRD of the SiO_2 powder reference, which gave the tridymite pattern.

Heat treatments at the crystallisation temperatures from DTA were applied to both PGN7 and PGN8 glasses. The crystallisation information is presented in Table 3 which shows that the same phases are formed in both glass-ceramics i.e. rhombohedral $Pb_2Nb_2O_7$, monoclinic $PbGeO_3$ and non indexed $PbGeO_3$. Monoclinic $PbNb_2O_6$ and hexagonal $Pb_5Ge_3O_{11}$ were not formed, underlining the difficulty in forming $Pb_5Ge_3O_{11}$–$PbNb_2O_6$ glass-ceramics from the PbO–GeO_2–Nb_2O_5 system. It has been reported[21] that the $PbNb_2O_6$ ferroelectric phase could only be obtained by quenching a pellet of rhombohedral $PbNb_2O_6$ from 1300 °C into ice-water. The melt temperature for this

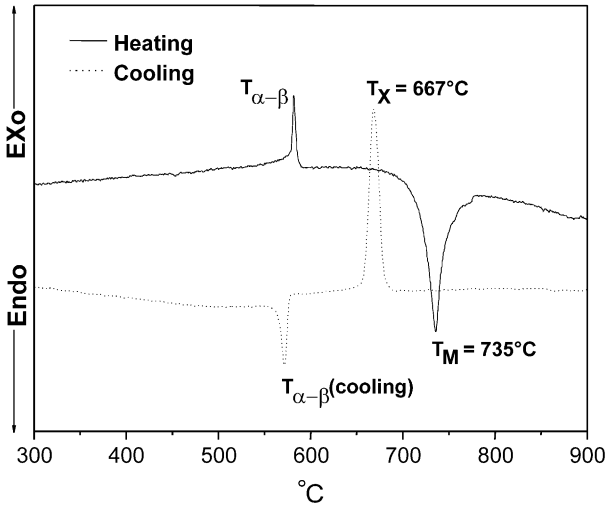

Fig. 6. DTA trace of as-quenched PGN2.

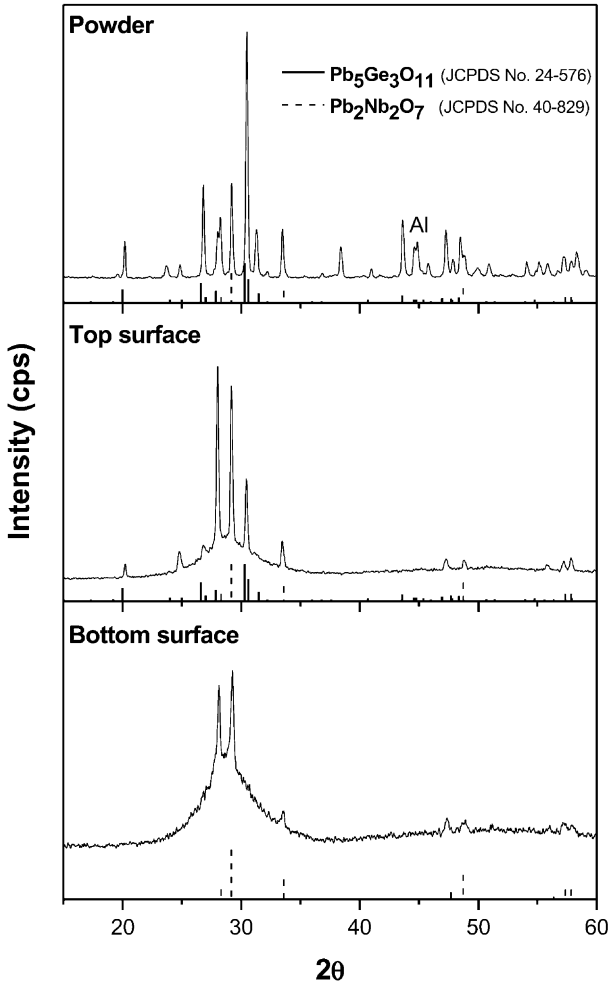

Fig. 5. X-ray diffraction patterns of as-quenched PGN2: powdered bulk, top surface and bottom surface. Peaks labelled Al are from the aluminium sample holder.

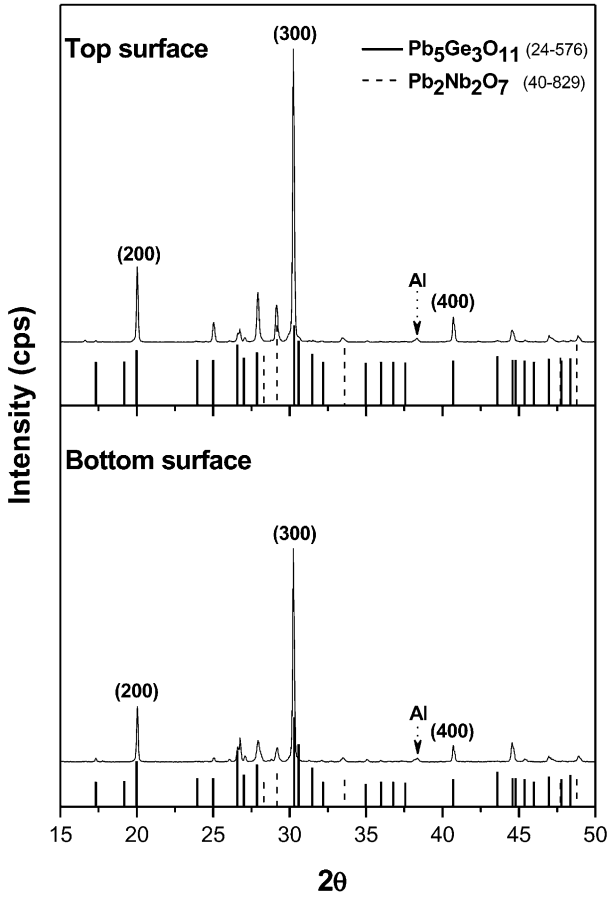

Fig. 7. X-ray diffraction patterns of the top surface and bottom surface of a PGN2 sample heat treated at 667 °C for 48 h. Peaks labelled Al are from the aluminium sample holder.

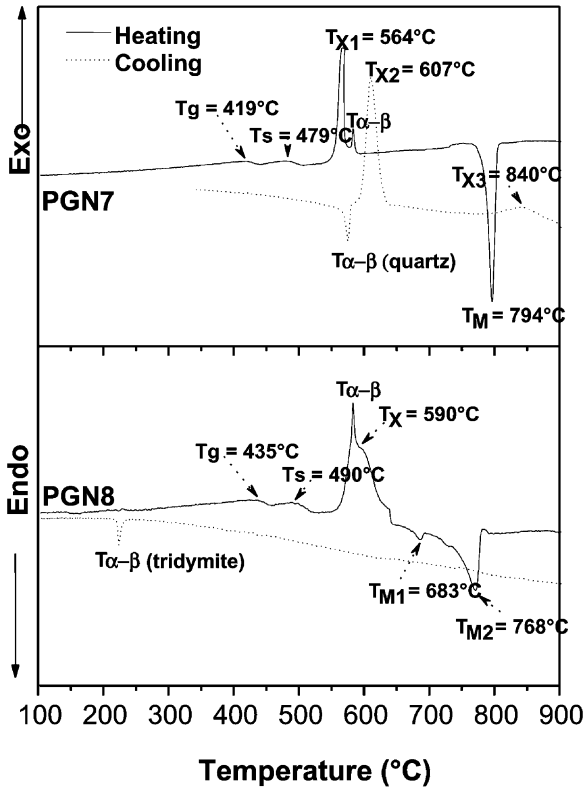

Fig. 8. DTA traces of PGN7 and PGN8.

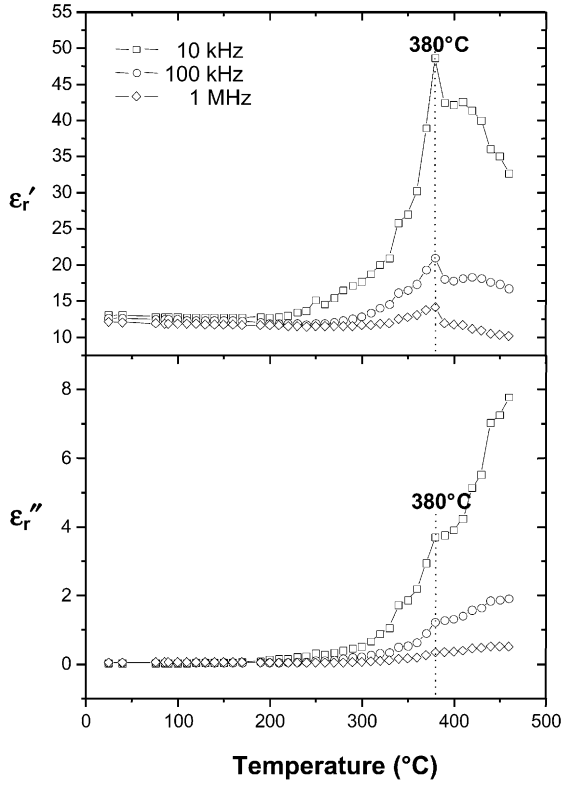

Fig. 9. Temperature dependence of the real (ε_r') and imaginary (ε_r'') parts of the complex permittivity of an as-quenched PGN2 sample, about 400±20 μm in thickness.

system was only between 1000 and 1150 °C. Therefore, it would be interesting to make these $Pb_5Ge_3O_{11}$–$PbNb_2O_6$ based glass-ceramics by adding some more refractory glass formers, such as SiO_2.

3.2.3. Dielectric measurement

Figs. 9 and 10 show the dielectric constants (ε_r') and dissipation factors (ε_r'') measured at 10 kHz, 100 kHz and 1 MHz of the PGN2 sample as-quenched and as-heat-treated respectively. In Fig. 9, there is a noticeable peak at about 380 °C at all frequencies. This is unlikely to be the Curie point of $Pb_5Ge_3O_{11}$ since its single crystal value is $T_C = 177$ °C. This sample was polished, before performing the dielectric measurement, until the thickness was reduced to about 420 μm. This would remove the $Pb_5Ge_3O_{11}$ phase from the top surface and the $Pb_2Nb_2O_7$ phase might now be dominant. Therefore, the peak at about 380 °C on the dielectric curves may be attributed to some transition of the $Pb_2Nb_2O_7$ phase, although there is no detectable peak in the DTA trace (Fig. 6). It is possible that the energy associated with this transition is very small. However, further study of this particular $Pb_2Nb_2O_7$ phase transition is needed.

From the dielectric parameters in Fig. 10, the curie point (T_C) of the PGN2 sample heat-treated at 667 °C for 48 h was observed to be about 166 °C, slightly lower than the single crystal value of 177 °C. This type of behaviour may be caused by two mechanisms: internal

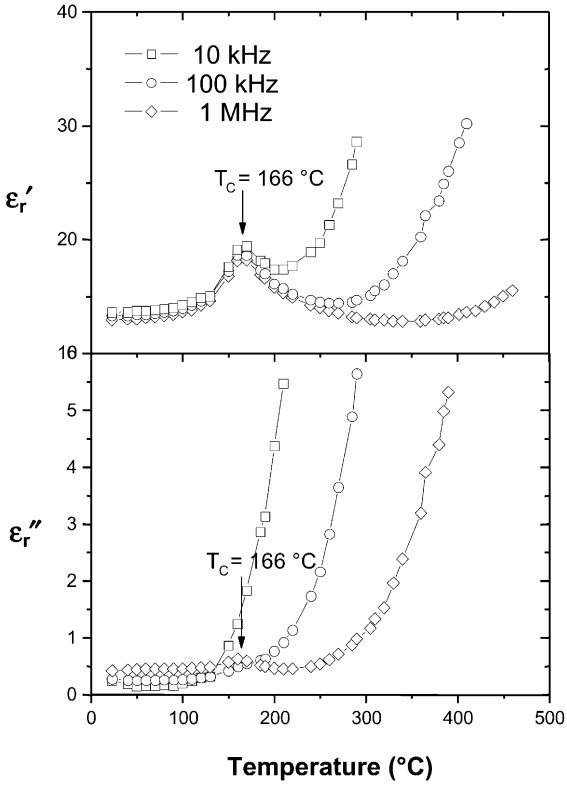

Fig. 10. Temperature dependence of the real (ε_r') and imaginary (ε_r'') parts of the complex permittivity of a PGN2 sample heat treated at 667 °C for 48 h and about 1400±20 μm in thickness.

Table 3
Thermal parameters, crystallisation temperatures and crystalline phases of glass-ceramics from PGN7 and PGN8 glasses

Sample	$T_g \pm 1$ (°C)	$T_s \pm 1$ (°C)	$T_m \pm 1$ (°C)	$T_x \pm 1$ (°C)	Crystalline phase
PGN7	419	479	794	564	$Pb_2Nb_2O_7$ (I), $PbGeO_3^{(II)}$, $PbGeO_3^{(III)}$
				From melt	$Pb_2Nb_2O_7^{(I)}$
PGN8	435	490	683768	590	$Pb_2Nb_2O_7$ (I), $PbGeO_3^{(II)}$, $PbGeO_3^{(III)}$

(I), (II) and (III) refer to JCPDS 40-829, 44-945 and 18-696 respectively.

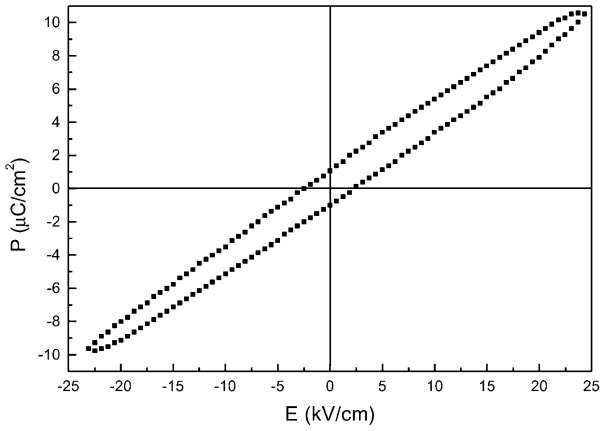

Fig. 11. Hysteresis loop at room temperature (50 Hz) from a PGN2 glass-ceramic of 260±20 μm thickness, heated at 667 °C for 48 h.

Table 4
Comparison of T_C (Curie temperature), P_s (spontaneous polarisation) and E_r (coercive field) of the PGN2 sample with some related ferroelectrics

Ferroelectrics	T_C (°C)	P_s (at room temperature) (μC/cm²)	E_r (kV/cm)
PGN2 (Glass-ceramic)	≈166	≈1	≈2.5
$Pb_5Ge_3O_{11}$ (Single crystal)	177	4.8	14
PG[25] (Thick film)	155–177	0.2–0.8	–

stress and impurities. The internal stresses may be attributed to small grain size, residual matrix or the combination of both.[22,23] However, if internal stress actually occurred, it would shift the XRD peaks, which was not observed. Therefore, the decrease in T_C may result from impurities because, according to Cornejo,[24] impurities in PG have a large effect in shifting T_C, especially when lead is replaced. At 1 MHz (room temperature), the dielectric constant (ε_r') of this sample was about 13, whereas that of the bulk $Pb_5Ge_3O_{11}$ sample from Cornejo and Haun[12] was about 27. The difference may be due to the different crystallographic orientations of the two samples or to the presence, in PGN2, of rhombohedral $Pb_2Nb_2O_7$.

3.3. Hysteresis loop

Hysteresis loops and electrical poling of the bulk PGN2 quenched sample were not achieved with electric fields up to 25 kV/cm. However, a PGN2 sample of 260 μm thickness, heat treated at 667 °C for 48 h, gave a ferroelectric hysteresis loop as shown in Fig. 11. This is to be expected since this heat treated sample contains a greater amount of the $Pb_5Ge_3O_{11}$ ferroelectric phase than the untreated sample. Table 4 shows a comparison of the important ferroelectric parameters of the heat-treated PGN2 sample and some related materials. The spontaneous polarisation value (Ps) at room temperature of PGN2 is quite small compared to that of a single crystal but slightly higher than the Ps value of the thick film $Pb_5Ge_3O_{11}$ (60 μm) with 28% *c*-axis orientation prepared by Takahashi et al.[25] They suggested that electric properties would be improved by increasing the fraction of c-plane orientation. However, the PGN2 heat treated sample exhibits *a*-axis orientation of the observed surface crystallisation, so giving a lower P_s value than the single crystal.

4. Conclusions

Among the ten compositions from $PbO–GeO_2–Nb_2O_5$ system only two compositions (PGN7 and PGN8) could be formed as glasses by the quenching method employed, leading to difficulty in obtaining a good parent glass for precipitating ferroelectric $Pb_5Ge_3O_{11}$ and $PbNb_2O_6$. By rapid quenching, a glass-ceramic containing ferroelectric $Pb_5Ge_3O_{11}$ and rhombohedral $Pb_2Nb_2O_7$ phase could be obtained from the PGN2 composition. SEM and XRD analysis confirmed the surface crystallisation of $Pb_5Ge_3O_{11}$, with *a*-axis orientation, and the bulk crystallisation of $Pb_2Nb_2O_7$. By heat treating at 667 °C for 48 h, $Pb_5Ge_3O_{11}$ could be grown further in this glass-ceramic with a higher degree of *a*-axis orientation. A non-saturated hysteresis loop was obtained from this heat treated sample, a consequence of the presence of $Pb_5Ge_3O_{11}$. However, the desired $PbNb_2O_6$ phase has not been observed, and $Pb_5Ge_3O_{11}–PbNb_2O_6$ based glass-ceramics have not been obtained from the $PbO–GeO_2–Nb_2O_5$ system.

Acknowledgements

The authors wish to thank Dr. David Hall, Dr. Jiang Quanzhong and Anuson Niyompan for their

continuous assistance throughout the dielectric and hysteresis loop measurements and K. Pengpat would like to record her thanks to the DPST project and Thai Government for financial support.

References

1. Canale, J. E., Condrate, R. A., Nassau, K. and Cornilsen, B. C., *Mater. Res. Soc. Symp. Proc.*, 1987, **88**, 169.
2. Iwasaki, H. and Sugii, K., *Appl. Phys. Lett.*, 1971, **19**(4), 92.
3. Nanamatsu, S., Sugiyama, H., Dor, K. and Kondo, Y., *J. Phys. Soc. Japan*, 1971, **31**, 616.
4. Sugii, K., Iwsaki, H. and Miyazawa, S., *Mater. Res. Bull.*, 1971, **6**, 503.
5. Iwata, Y., Koizumi, H., Koyano, N., Shibuya, I. and Niizeki, N., *J. Phys. Soc. Jpn.*, 1973, **35**, 314.
6. Iwata, Y., Koyano, N. and Shibuya, I., *J. Phys. Soc. Jpn.*, 1973, **35**, 1269.
7. Hasegawa, H., Shimada, M. and Koizumi, M., *J. Mater. Sci.*, 1973, **8**, 2923.
8. Schmitt, H. and Kleer, G., *Mater. Res. Bull.*, 1985, **20**, 829.
9. Ying, X. L. and Chen, L. J., *Prog. Crystal Growth and Charact*, 1985, **11**, 237.
10. Kim, J. H., Kim, J. B. and Lee, K. S., *Solid State Commun.*, 1993, **88**, 727.
11. Kageyama, Y., Sakata, J. and Taga, Y., *Jpn J. Appl. Phys*, 1995, **34**, 5158.
12. Cornejo, A. I. and Haun, M. J., *Mater. Res. Soc. Symp. Proc.*, 1996, **400**, 353.
13. Eysel, W., Wolfe, R. W. and Newnham, R. E., *J. Am. Ceram. Soc.*, 1973, **56**(4), 185.
14. Topping, J. A., Fuchs, P. and Murthy, M. K., *J. Am. Ceram. Soc.*, 1974, **57**(5), 205.
15. Hasegawa, H., Shimada, M., Kanamaru, F. and Koizumi, M., *Bull. Chem. Soc. Jpn.*, 1977, **50**(2), 529.
16. Hasegawa, H., Shimada, M. and Koizumi, M., *Ceram. Int.*, 1982, **8**(4), 141.
17. Sawyer, C. B. and Tower, C. H., *Phys. Rev.*, 1930, **57**, 54.
18. Glazer, A. M., Groves, P. and Smith, D. T., *J. Phys. E:Sci Instruments*, 1984, **17**, 95.
19. Mazurin, O. V., Streltsina, M. V., Shvsiko-Shvaikovskaya, T. P. *Handbook of Glass Data, Part D: ternary non-silicate glasses*. Elsevier, Oxford, 1991.
20. Nassau, K., *J. Non. Cryst. Solids*, 1980, **42**, 423.
21. Lee, H. S. and Kimura, T., *J. Am. Ceram. Soc.*, 1998, **81**(12), 3228.
22. Grossman, D. G. and Isard, J. O., *Mater. Sci.*, 1969, **4**, 1059.
23. Herczog, A., *J. Am. Ceram. Soc.*, 1964, **47**(3), 107.
24. Cornejo, I. A. 1994, Ph.D. Thesis, T-4631, Colorado School of Mines, Golden, Co, USA.
25. Takahashi, K., Ueda, H., Suzuki, T. and Kakegawa, K., *Ferroelectric*, 1994, **154**, 41.